Plant Physiology®

Plant Physiology, 2024, 195, 2668–2682
https://doi.org/10.1093/plphys/kiae239
Advance access publication 15 May 2024
Research Article

Isohydricity and hydraulic isolation explain reduced hydraulic failure risk in an experimental tree species mixture

Myriam Moreno,[1,2,*] Guillaume Simioni,[1] Hervé Cochard,[3] Claude Doussan,[4] Joannès Guillemot,[5,6,7] Renaud Decarsin,[1] Pilar Fernandez-Conradi,[1] Jean-Luc Dupuy,[1] Santiago Trueba,[8] François Pimont,[1] Julien Ruffault,[1] Frederic Jean,[1] Olivier Marloie,[1] and Nicolas K. Martin-StPaul[1]

[1]Unité de Recherche en écologie des Forêts Méditerranéennes, INRAE, 84914 Avignon, France
[2]French Environment and Energy Management Agency, 49000 Angers, France
[3]Physique et physiologie Intégratives de l'Arbre en environnement Fluctuant, INRAE, Université Clermont Auvergne, 63000 Clermont-Ferrand, France
[4]Environnement Méditerranéen et Modélisation des Agro-Hydrosystèmes, INRAE, 84914 Avignon, France
[5]UMR Eco&Sols, CIRAD, 34398 Montpellier, France
[6]Eco&Sols, Univ Montpellier, CIRAD, INRAE, IRD, Montpellier SupAgro, 34398 Montpellier, France
[7]Department of Forest Sciences, ESALQ, University of São Paulo, 13418-900 Piracicaba, São Paulo, Brazil
[8]Biodiversité Gènes et Communautés, INRAE, Université de Bordeaux, 33615 Pessac, France
*Author for correspondence: myriam.moreno@inrae.fr
The author responsible for distribution of materials integral to the findings presented in this article in accordance with the policy described in the Instructions for Authors (https://academic.oup.com/plphys/pages/General-Instructions) is Myriam Moreno (myriam.moreno@inrae.fr).

Abstract

Species mixture is promoted as a crucial management option to adapt forests to climate change. However, there is little consensus on how tree diversity affects tree water stress, and the underlying mechanisms remain elusive. By using a greenhouse experiment and a soil-plant-atmosphere hydraulic model, we explored whether and why mixing the isohydric Aleppo pine (*Pinus halepensis*, drought avoidant) and the anisohydric holm oak (*Quercus ilex*, drought tolerant) affects tree water stress during extreme drought. Our experiment showed that the intimate mixture strongly alleviated *Q. ilex* water stress while it marginally impacted *P. halepensis* water stress. Three mechanistic explanations for this pattern are supported by our modeling analysis. First, the difference in stomatal regulation between species allowed *Q. ilex* trees to benefit from additional soil water in mixture, thereby maintaining higher water potentials and sustaining gas exchange. By contrast, *P. halepensis* exhibited earlier water stress and stomatal regulation. Second, *P. halepensis* trees showed stable water potential during drought, although soil water potential strongly decreased, even when grown in a mixture. Model simulations suggested that hydraulic isolation of the root from the soil associated with decreased leaf cuticular conductance was a plausible explanation for this pattern. Third, the higher predawn water potentials for a given soil water potential observed for *Q. ilex* in mixture can —according to model simulations—be explained by increased soil-to-root conductance, resulting from higher fine root length. This study brings insights into the mechanisms involved in improved drought resistance of mixed species forests.

Introduction

The rising frequency and intensity of extreme droughts are impacting tree survival and forest functions worldwide (Allen et al. 2010; Breshears et al. 2013; Senf et al. 2020), jeopardizing crucial forest ecosystem services. Tree species diversity has been promoted as an important nature-based solution to improve the resilience of forests and tree plantations (Messier et al. 2022). The effects of species mixing on drought resistance could result from different mechanisms, such as competitive reduction for water through resource partitioning or facilitation—for instance hydraulic redistribution (Grossiord 2020). Yet, tree species diversity effects on tree drought resistance are not universal and can change in direction and magnitude according to the sites, the species of the composition of the mixture (Grossiord 2020; Grossiord et al. 2014b; Mas et al. 2024). Indeed, previous studies showed that tree species diversity effect can have positive (Lebourgeois et al. 2013; de-Dios-García et al. 2015; Ruiz-Benito et al. 2017), neutral (Grossiord et al. 2014b; Merlin et al. 2015), or even negative impacts (Grossiord et al. 2014a; Vitali et al. 2018). These conflicting results suggest that it is not the species richness that matters but rather the functional composition of the mixtures (i.e. the association of species with different drought response strategies; Forrester and Bauhus 2016; Grossiord 2020). This hypothesis was supported by recent research that found that the diversity of hydraulic traits determines the resilience to drought of forest water fluxes globally (Anderegg et al. 2018). Similarly, results from a large-scale tree diversity experiment showed that the diversity of drought resistance strategies is a good predictor of the stability of tree growth and forest productivity (Schnabel et al. 2021). However, we crucially miss a mechanistic understanding of the way the diversity of drought resistance strategies mediates tree mortality under extreme drought.

Received January 31, 2024. Accepted March 27, 2024.

Tree species drought resistance strategies result from a set of functional traits that determine how rapidly plant water status (often quantified as water potential) crosses vital physiological thresholds. In particular, drought resistance strategies determine the loss of hydraulic conductance caused by a high rate of embolism in xylem conduits (Tyree and Sperry 1989), i.e. the risk of xylem hydraulic failure, a leading mechanism in drought-induced tree mortality (Adams et al. 2017; Sanchez-Martinez et al. 2023).

It is common in the literature to distinguish species drought resistance strategies based on the water loss regulation through stomatal closure (Klein 2014; Martin-StPaul et al. 2017) and the xylem vulnerability to embolism (Delzon 2015; Choat et al. 2018; Martin-StPaul et al. 2017). Isohydric species (sometimes also referred as drought avoidant) close their stomata relatively early during drought and have a lower cuticular conductance. Therefore, they limit soil water depletion, which in turn limits the soil and plant water potential decrease and the overall risk of hydraulic failure (Delzon 2015; López et al. 2021). They also tend to have relatively narrow safety margins and are less embolism resistant than anisohydric species. Anisohydric species (also referred as drought tolerant) have higher resistance to drought-induced xylem embolism. However, they tend to maintain gas exchanges during drought via a delayed stomatal regulation and relatively higher cuticular conductance. This implies greater soil water depletion and greater drop in soil and plant water potential during drought (Martin-StPaul et al. 2017; Choat et al. 2018; Fig. 1A).

Based on this knowledge, one can hypothesize how mixing 2 species with such distinct drought response strategies will impact soil water dynamic, plant water status (water potentials), and the risk of hydraulic failure under extreme drought. To facilitate the reasoning, we assume that trees are hydraulically connected to the soil (i.e. soil and plant predawn water potential are very close) and that the root systems of both species are intimately mixed and fully occupy a given soil volume. We can then derive 3 complementary hypotheses (which are also depicted in Fig. 1B):

1. For an anisohydric (drought-tolerant) species, it is beneficial to compete for water with an isohydric (drought-avoidant) neighbor. Indeed, the soil water saved by earlier stomatal regulation of the isohydric is available to maintain gas exchanges and delay the decrease in water potential and the overall hydraulic failure risk (Fig. 1B).
2. By contrast, mixing is detrimental to an isohydric (drought-avoidant) species, as it experiences lower soil water potential due to sustained water use by the companion anisohydric species. This leads to a decrease in its water potential, thereby increasing the risk of hydraulic failure. The scenario presented in Fig. 1B—which shows that an anisohydric always "wins the fight" during drought under mixture—holds only if the predawn water potential of the mixed species is at equilibrium with the soil water potential.
3. If the root systems of the 2 neighbors species are segregated in space, water consumption by the anisohydric species does not affect the isohydric species, and differences in water potentials between tree species in the mixture could occur given their spatial isolation (Fig. 1B). In support to this hypothesis, root niche separation is often proposed as a mechanism allowing to reduce water stress for trees associated in mixture (Jose et al. 2006; Grossiord 2020).

In this study, we combined a greenhouse experiment and a mechanistic model analysis to evaluate these hypotheses and explore the mechanisms and traits involved in the modulation of water stress in mixed forests during an extreme drought. We compared the ecophysiological responses to drought of holm oak (*Quercus ilex*) and Aleppo pine (*Pinus halepensis*) grown in monocultures and in mixtures. In order to evaluate the importance of having root systems intimately mixed, we also added a treatment in which the root systems of the 2 plants were separated (Fig. 1B).

Results

Water status dynamic in the different treatments

Soil water content, soil water potential (Ψ_{soil}), and plant predawn water potential (Ψ_{pd}) declined during drought for both species and in all pot compositions (Fig. 2A, Supplementary Fig. S1). In accordance, soil electrical resistivity increased during drought (Supplementary Fig. S2). However, the temporal dynamics differed between species, in agreement with their drought response strategies (Moreno et al. 2021). Ψ_{pd} decline was more pronounced for the anisohydric *Q. ilex*, which exhibited Ψ_{pd} as low as −8 MPa, than for the isohydric *P. halepensis*, for which Ψ_{pd} did not go below −4 MPa regardless of the pot composition (Fig. 2A, Supplementary Table S1 with $P < 0.001$ for the species effect). Gas exchanges also decreased for the 2 species (Supplementary Fig. S3, $P > 0.05$) for all pot compositions, but the decrease tended to occur earlier for the isohydric *P. halepensis* than for the anisohydric *Q. ilex* (Supplementary Fig. S3).

For *Q. ilex*, our empirical data suggested a positive effect of mixture (without separation) on drought stress at the early stage of drought as leaf gas exchanges tended to be slightly higher in mixture than in monoculture at the second date of measurements (Supplementary Fig. S3). This trend was confirmed during extreme drought (latest date of the experiment) on plant water potential (Fig. 2A), which was significantly higher in mixture than in monoculture (mean Ψ_{pd} of −6.37 MPa in mixture against mean Ψ_{pd} of −8.3 MPa in monoculture; Supplementary Table S2, $P < 0.01$ for the date:mixture interaction effect). At the drought peak, this water potential difference between treatments translated into a significant effect on hydraulic safety margins (mean HSM = Ψ_{pd} − P50, an indicator of the risk of hydraulic failure), which was higher in mixture (mean HSM = 0.73 MPa) than in monoculture (mean HSM = −1.33 MPa) *for Q. ilex* (Fig. 2B, $P < 0.05$). For *P. halepensis*, there was a trend toward lower gas exchange in mixture during early drought (Supplementary Fig. S3). However, during extreme drought, we found no significant difference in plant water potential (Supplementary Table S2, $P > 0.05$ for the date:mixture interaction effect) between treatments, and thus, for HSM (Fig. 2B, $P > 0.05$; mean HSM = 1.1 MPa in mixture and 1.43 MPa in monoculture).

For both species, plants grown in mixture with a root separation treatment exhibited no significant difference with monoculture for gas exchange or plant water potential. This indicates that mixture only had an effect on water stress if tree root systems were intimately entangled. This result was supported by an analysis showing that water flow from one compartment to the other of the pot equipped with a mesh (i.e. through the mesh) during drought is very limited (Supplementary Method S1 and Table S3). In brief, we applied Darcy's law for different types of soil textures using water potential gradient as the difference in predawn water potential between the 2 species at the penultimate and last dates of measurements (largest water potential gradient measured for the experiment). We found that water flow occurring between the 2 plant species through the mesh was very low, and negligible compared to the transpiration flow, due to the very sharp decline in soil hydraulic conductivity.

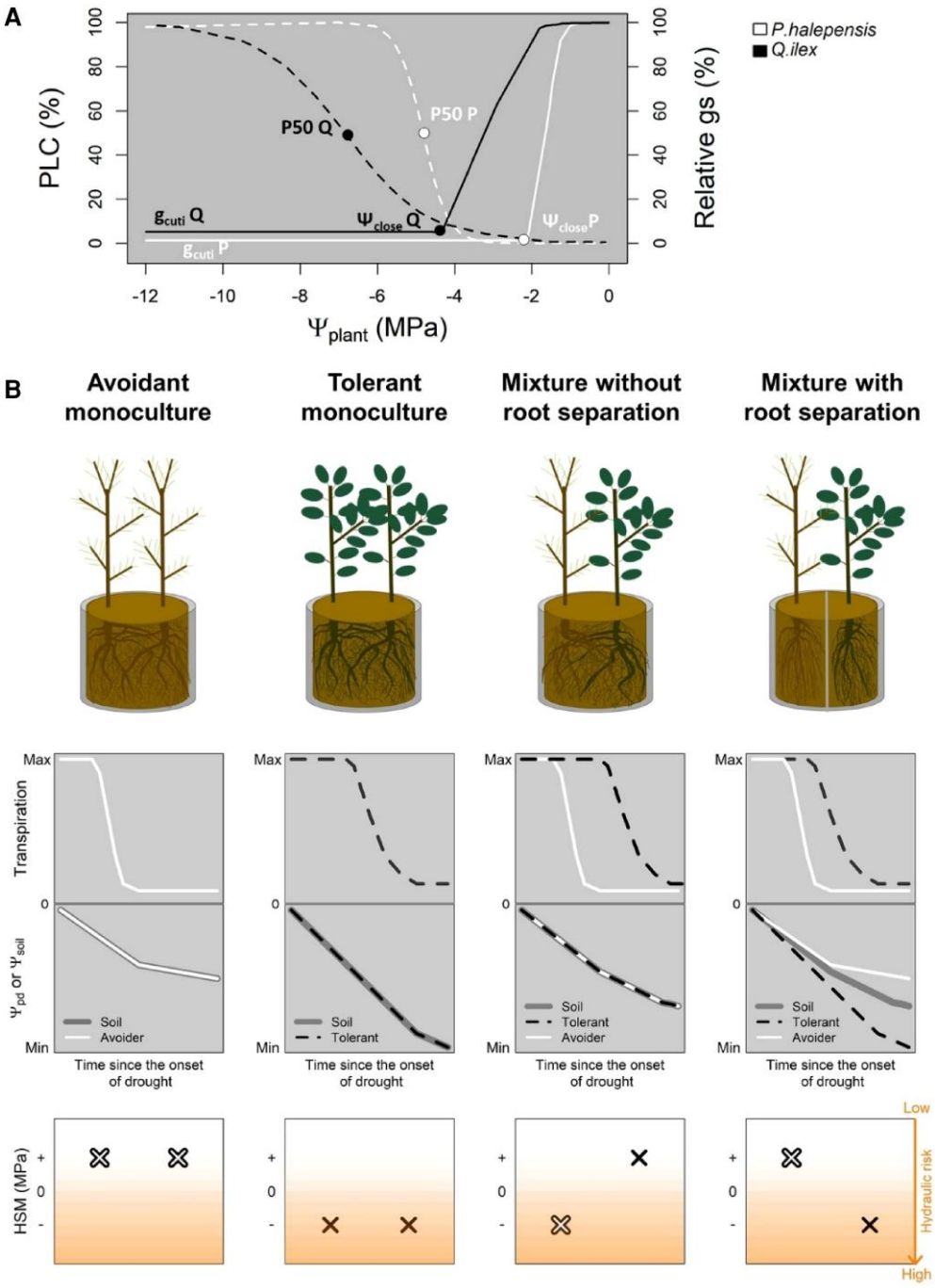

Figure 1. Conceptual representation of drought effects on hydraulic risk of monocultures and mixtures, for 2 species with contrasting water use strategies. **A)** Drought responses of species according the resistance strategy they adopt. During drought, the *isohydric* species (i.e. *P. halepensis*, also referred as drought avoidant) close its stomata at a relatively high-water potential (Ψ_{close}, corresponding to the water potential inducing full stomatal closure) and have a low cuticular conductance (g_{cuti}). Also, it has a relatively high P50 (water potential causing 50% loss of hydraulic conductivity), making it more vulnerable to xylem cavitation, whereas the *anisohydric* species (i.e. *Q. ilex*, also referred as drought tolerant) has a lower Ψ_{close} and a higher g_{cuti}, making it consuming more water. Additionally, it has a lower P50 (water potential causing 50% loss of hydraulic conductivity), making it more resistant to xylem cavitation. **B)** Experimental design and hypothesized drought responses for monocultures and mixtures of an *isohydric* (drought-avoidant) and an *anisohydric* (drought-tolerant) species. The transpiration, water potentials (Ψ_{soil}: overall pot soil water potential; Ψ_{pd}: plant predawn water potential), and hydraulic safety margins (HSM) for each situation and species. HSM represents the risk of hydraulic failure, and it generally refers as the difference between the minimum plant water potential and vulnerability to cavitation (P50, the water potential causing 50% of embolism). In the *isohydric* monoculture, tree transpiration is expected to reduce rapidly after the onset of drought, limiting the drop in Ψ_{soil} and Ψ_{pd}, and hence the hydraulic failure risk (positive HSM). In the *anisohydric* monoculture, transpiration should decrease later as stomatal control is expected to be more released than the one of the isohydric species. This should trigger a steeper decrease of Ψ_{soil} and Ψ_{pd}, thereby increasing the risk of hydraulic failure (more negative HSM). In the mixture without root separation, transpiration of the *isohydric* should decrease earlier than for the *anisohydric*. This is expected to dampen overall soil water loss and thus Ψ_{pd} and HSM of the *anisohydric* species compared to the monoculture. However, the water consumption of the *anisohydric* continues beyond the point of stomatal closure and of cavitation of the *isohydric*. This triggers a decrease of steeper decline of Ψ_{pd} and HSM for the *isohydric* compared to monoculture. A mixture with root separation illustrates that when each species root system occupies its proper soil volume, the regulation of the transpiration, the water potential dynamics, and the HSM are expected to be the same as in monoculture. As Ψ_{soil} represents the global pot soil water potential, it is here equal to the mean of both compartment soil water potentials.

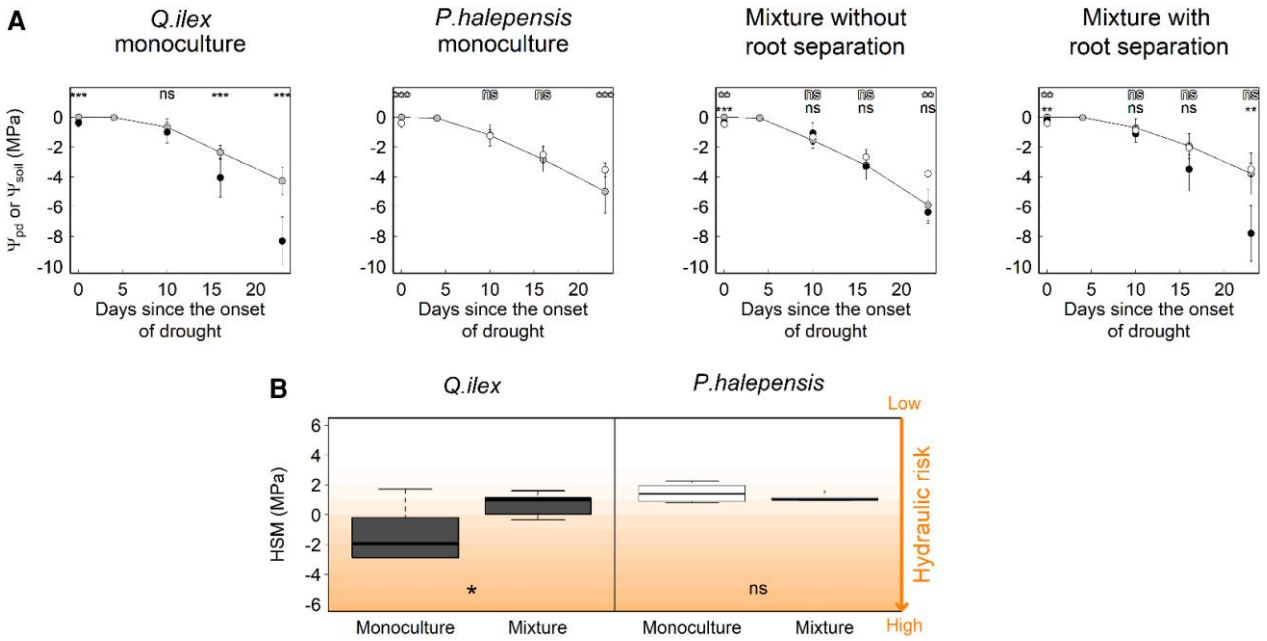

Figure 2. Drought impact on water potential and hydraulic risk according to species mixture and root separation. **A)** Soil (Ψ_{soil}) and leaf predawn water potentials (Ψ_{pd}) for the different pot compositions at each measurement date. Ψ_{soil} represents average values computed at the pot level from manual weightings (gray points). The average Ψ_{pd} of *Q. ilex* and *P. halepensis* correspond respectively to black and white dots. SD are represented, and significant differences between Ψ_{soil} and Ψ_{pd} obtained using Student's *t* tests are indicated (ns, nonsignificant difference; *, $0.01 \leq P\_value < 0.05$; **, $0.001 \leq P\_value < 0.01$; ***, $P\_value < 0.001$). For Ψ_{pd}, $N = 24$ for monocultures (pooling monocultures with and without root separation/2 trees per pots) and 6 for mixtures. For Ψ_{soil}, $N = 12$ for monocultures (pooling monocultures with and without root separation) and 6 for mixtures. **B)** Hydraulic safety margins (HSM) measured at the driest date of the experiment in monocultures (with and without root separation) and the mixture without root separation. HSM were computed as the difference between Ψ_{pd} at the driest date and the P50 (i.e. Ψ_{pd} causing 50% embolism, see Table 4 for P50 values used for each species). Significant differences between HSM according to species and pot modalities were obtained using Student's *t* tests and are indicated (ns, nonsignificant difference; *, $0.01 \leq P\_value < 0.05$). $N = 24$ for monocultures (pooling monocultures with and without root separation/2 trees per pots) and 6 for mixtures. Boxes represent the median, 25th, and 75th percentiles, error bars the 10th and 90th percentiles, and dots outliers.

Modification of the plant vs. soil water potential relationship in mixture

During the beginning of the drought, Ψ_{pd} and Ψ_{soil} were very close for both species (Figs. 2A and 3A) in all treatments. However, as drought gradually increased, Ψ_{pd} and Ψ_{soil} differed progressively for both species and in all treatments except for *Q. ilex* in mixture (Figs. 2A and 3A). The slope of the Ψ_{pd} vs. Ψ_{soil} relationship differed between species (Fig. 3A). Whereas Ψ_{pd} became lower than Ψ_{soil} for *Q. ilex* with increasing drought, Ψ_{pd} became higher than Ψ_{soil} for *P. halepensis*. Such observation remained significant even when considering the uncertainty in calculating Ψ_{soil} (Supplementary Fig. S4). The fact that Ψ_{soil} was more negative than Ψ_{pd} for *P. halepensis* in the monoculture suggests that some soil evaporation occurred, due to imperfect covering of the pots or to the holes made in the pots for the drainage of water and the measurement of soil resistivity. A peculiar pattern was found for *Q. ilex* in mixtures (without root separation), for which Ψ_{pd} equaled Ψ_{soil} all along the desiccation dynamic (Fig. 3A and Table 1, $P = 2.12e^{-07}$ for the Ψ_{soil}: pot modalities effect). Indeed, the slope of the relationship between Ψ_{pd} and Ψ_{soil} for *Q. ilex* in mixtures without root separation was close to 1, but was 1.74 for the other pot modalities (Table 2, $P < 0.001$ for the Ψ_{soil}: mixture without root sep interaction).

Changes in the behavior of *Q. ilex* in mixture were further confirmed by exploring the relationship between the Ψ_{pd} of the 2 species in mixtures with and without root separation (Fig. 3B). We found a significantly lower slope (slope = 1.6) in the mixture without root separation than in the mixture with root separation (slope = 2.21; Fig. 3B and Table 3, $P = 0.03$ for the species × separation modality interaction).

Results of the model simulations and sensitivity analysis

Figure 4 shows simulation results with the SurEau model for water potential and transpiration under "benchmark" conditions (i.e. traits were set according to the hypothesis formulated in Fig. 1B). In these simulations, the anisohydric (*Q. ilex*) exhibited an increase transpiration by 20% and experienced later time to hydraulic failure (THF; increased by a factor of 1.5 in mixture compared to monoculture). On the contrary, the isohydric species (*P. halepensis*) showed a reduction of transpiration by ca. 20% and an earlier THF twice shorter in mixture than in monoculture. In addition, Ψ_{pd} (maximal daily Ψ_{plant}, taken at night) and Ψ_{soil} were always very close to each other until significant loss of plant hydraulic conductance occurred.

These simulations were consistent with the hypotheses drawn in Fig. 1B, but not with the experimental results (Fig. 2). Simulations departed from our empirical findings on 2 points. Simulations showed (i) greater water stress for *P. halepensis* in mixture and (ii) a tight relationship between Ψ_{pd} and Ψ_{soil}, for the 2 species.

We conducted different sensitivity analyses (Fig. 5) to further understand the reasons underpinning the departure between model and experimental data.

First, we tested if plant isolation (i.e. "hydraulic decoupling") could match the empirical data (i.e. higher Ψ_{pd} than Ψ_{soil}) during drought for the isohydric *P. halepensis*. We first implemented a root-to-soil hydraulic isolation by applying a decrease in root hydraulic conductance (K_{root}) as Ψ_{plant} declines (Supplementary Fig. S5). This did not allow to simulate higher Ψ_{pd} than Ψ_{soil} for

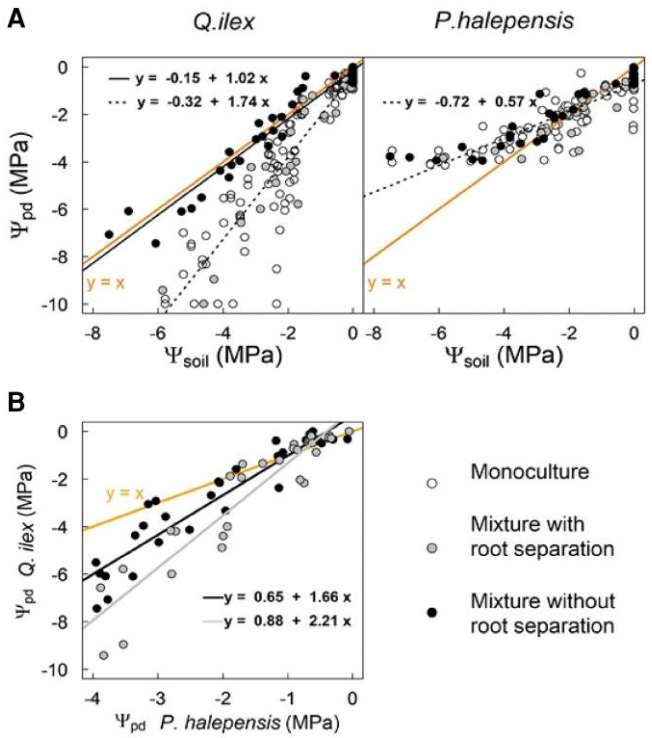

Figure 3. Mixture effect on the hydric behaviors of *Q. ilex* and *P. halepensis*. **A)** Relationships between soil (Ψ_{soil}) and predawn (Ψ_{pd}) water potentials of *Q. ilex* and *P. halepensis* in mixtures with root separation, without root separation, and monocultures. The isoline ($y = x$) is reported in orange. Distinct linear fits between Ψ_{soil} and Ψ_{pd} are depicted for significantly different relationships (see Table 2), and the corresponding equations are given. For *Q. ilex*, fit between Ψ_{soil} and Ψ_{pd} combining both monoculture and mixture is represented in dashed line and in solid black line for mixture without root separation. For *P. halepensis*, fit between Ψ_{soil} and Ψ_{pd} combines all 3 pot modalities. $N = 96$ for monocultures (with and without root separation) and 24 for mixtures for each root separation category. **B)** Relationships between predawn water potentials (Ψ_{pd}) of *Q. ilex* and *P. halepensis* in mixtures with root separation and without root separation. $N = 24$ for each root separation category. Summary statistics are shown in Table 3.

this species (Fig. 5A, variable K_{root}). Second, we implemented a leaf to air hydraulic isolation by implementing a decrease of the leaf cuticular conductance (g_{cuti}; i.e. isolation from air dryness, Supplementary Fig. S6A) with decreasing leaf relative water content (RWC), in accordance with empirical data obtained in *P. halepensis* using the DroughtBox method (Billon et al. 2020; Supplementary Fig. S6B). The results showed that reducing only g_{cuti} did not allow to match the empirical pattern ($\Psi_{pd} > \Psi_{soil}$, Fig. 5A, variable g_{cuti}). In a third simulation, we implemented both a decrease of K_{root} and a decrease of g_{cuti} during drought stress. This allowed to simulate a greater survival in mixture than in monoculture (similar THF), and $\Psi_{pd} > \Psi_{soil}$ in accordance with empirical results (Fig. 5A, variables K_{root} and g_{cuti}). These tests support that hydraulic isolation can be a way for pine to maintain a constant hydraulic risk during increasing drought even in mixture with anisohydric oak.

Secondly, to explain the change in the Ψ_{pd} to Ψ_{soil} relationship observed for *Q. ilex* in our empirical data (Fig. 3A and Table 1, $P = 2.12e^{-07}$ for the Ψ_{soil}: pot modalities effect), we tested the hypothesis of an enhanced soil hydraulic conductance in mixture, through increased fine root length (Equations 3 and 4 in the Materials and methods section). This would be consistent with the observation of greater root length in mixture (Supplementary Fig. S7). Simulation

Table 1. *F* statistics and *P* values of factors in the ANOVA model of the predawn water potentials of both species according to pot modalities (monoculture or mixture, with or without root separation) and soil water potentials (Ψ_{soil})

	Q. ilex		*P. halepensis*	
Factors	**F_value**	**P_value**	**F_value**	**P_value**
Ψ_{soil}	824.83	$<2.2e^{-16}$	707.69	$<2.2e^{-16}$
Pot modalities	30.24	$11.38e^{-11}$	1.84	0.1
Ψ_{soil}: pot modalities	17.26	$2.12e^{-07}$	1.89	0.15

Table 2. Summary of linear mixed effect model of the predawn water potentials of both species according to pot modalities (monoculture mixture with or without root separation) and soil water potentials (Ψ_{soil}) using monoculture as reference

	Q. ilex		*P. halepensis*	
Factors	**T_value**	**P_value**	**T_value**	**P_value**
Intercept	−1.489	0.139	−7.904	$1.3e^{-12}$
Ψ_{soil}	25.77	$<2e^{-16}$	21.318	$<2e^{-16}$
Mixture with root sep	0.03	0.98	0.06	0.95
Mixture without root sep	0.63	0.53	0.21	0.83
Ψ_{soil}: mixture with root sep	0.32	0.75	1.77	0.08
Ψ_{soil}: mixture without root sep	−5.64	$9.71e^{-08}$	−0.45	0.65

results showed that increasing soil hydraulic conductance allowed Ψ_{plant} to keep closer to Ψ_{soil} during drought (Fig. 5B).

Discussion

It has been hypothesized that competition for water during drought is reduced between species with contrasting hydraulic strategies (isohydric vs. anisohydric) in mixtures (Anderegg et al. 2018; Bello et al. 2019; Schnabel et al. 2021; Haberstroh and Werner 2022). However, very little is known about how species interactions affect tree resistance to extreme drought (Grossiord 2020; Haberstroh and Werner 2022), and experimental test comparing monocultures and mixtures of species with contrasting hydraulic strategies during extreme drought are lacking. The extreme drought experiment that we conducted in a greenhouse highlighted that mixing an isohydric and an anisohydric species strongly alleviated the water stress of the anisohydric species, while it had a relatively weak impact on the water stress of the isohydric species (Fig. 2). This result is only partially in agreement with the initial hypotheses drawn in Fig. 1B and with the benchmark model simulations that were based on these hypotheses (Fig. 4). Our data and model analyses helped to identify 3 mechanistic explanations for these results: (i) the differences in water use strategy between the 2 species, (ii) the ability of *P. halepensis* to isolate (or disconnect) during drought, and (iii) the changes in the soil hydraulic conductance possibly related to fine root density. These mechanisms are discussed in the following.

Differences in water use strategy partly explain the mixture effect on gas exchanges and hydraulic risk

Experimental data supported that *Q. ilex* could maintain gas exchange longer and experienced lower hydraulic risk during drought in the "true mixture" (i.e. pots designed without root separation) than in the monoculture (Fig. 2, Supplementary Fig. S3). This pattern is in agreement with our initial hypothesis

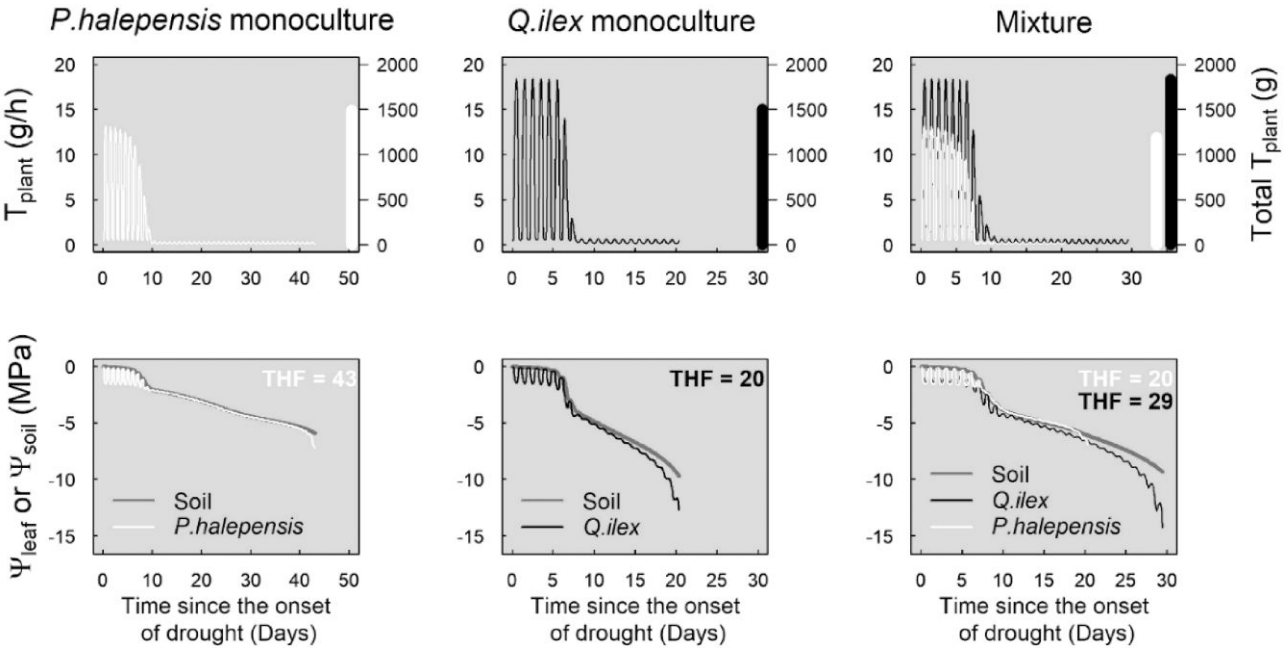

Figure 4. SurEau model simulations in monocultures and mixture (refer to as Benchmark simulations in the text). Upper panels show the simulated dynamics of transpiration (T_{plant}, in g/h) and the total tree transpiration until hydraulic failure (Total T_{plant}, in g). Lower panels show the leaf (Ψ_{leaf}) and soil (Ψ_{soil}) water potentials. The time to reach hydraulic failure (THF, corresponding to the number of days to reach 100% loss in hydraulic conductivity) is indicated for *P. halepensis* and *Q. ilex*, respectively, for the different composition treatments.

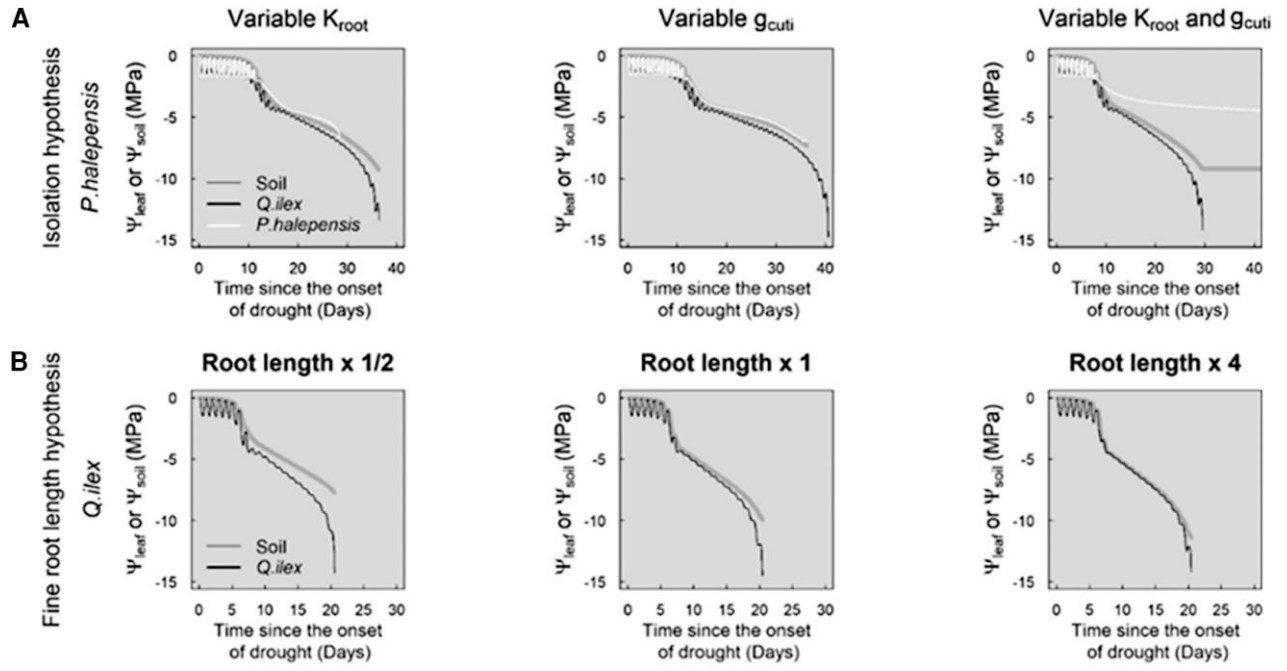

Figure 5. Sensitivity analysis with the SurEau model to explore the role of K_{root}, g_{cuti}, and K_{soil} (which is modified through the fine root length) on the changes of the relationship between soil water potential (Ψ_{soil}) and plant water potential (Ψ_{leaf}). **A)** Test of sensitivity to root conductance (K_{root}) and leaf cuticular conductance (g_{cuti}) parameters for *P. halepensis*. **B)** Test of sensitivity to fine root length for *Q. ilex* (fine root length multiplied by 1/2, 1, and 4 compared to the benchmark). Note that the scales of the x axis differ between plots. Model parameters are provided in the Tables 4 and 5.

H1 (Fig. 1B) and with previous assumptions of the literature (Bello et al. 2019; Mas et al. 2024). In addition, such empirical results were confirmed by the SurEau simulations under benchmark conditions, that were fully in line with our initial hypothesis (Fig. 4). For *P. halepensis*, lower gas exchanges during early drought were measured in the "true mixture" than in the monoculture. This is also consistent with our initial assumption and with SurEau model simulations under benchmark conditions. The most straightforward explanation for these results is the difference in stomatal behavior between the 2 species, which has been proposed in the introduction: during drought, it is beneficial for an anisohydric species (such as *Q. ilex*) to compete with an isohydric (such as *P. halepensis*) because the earlier stomatal regulation of the isohydric saves some water, which is made available

to the anisohydric to maintain gas exchanges and delay the decrease in water potential and the overall hydraulic failure risk. On the contrary, for the isohydric species, being in mixture with an anisohydric would trigger an earlier drought stress and water loss regulation.

However, different experimental results departed from the initial assumptions and from the SurEau simulations under benchmark conditions, suggesting that additional effects were at play in the interspecific interaction. Firstly, for *P. halepensis*, no difference in predawn water potential between monoculture and mixture was found during extreme drought. More importantly, this species was able to maintain a predawn water potential higher than the soil water potential as commonly found in the field (e.g. Moreno et al. 2021), which suggests that this species can limit its desiccation and maintain water status through some form of hydraulic disconnection. For *Q. ilex*, we found a change in the relationship between predawn water potential and soil water potential in mixture compared to monoculture (Fig. 3), supporting that this species can maintain higher predawn water potential for a given level of soil drought in mixture. This is disussed in the third section of this discussion.

Hydraulic disconnection ("isolation hypothesis") of the isohydric *P. halepensis* as a mean to limit hydraulic risk in mixture during drought

The fact that *P. halepensis* exhibited higher Ψ_{pd} than Ψ_{soil} during drought when grown in mixture with *Q. ilex* (Fig. 2) contradicts our initial hypothesis (Fig. 1B) and the model simulations under benchmark conditions (Fig. 4). An explanation for this is the ability of this species to (i) disconnect (or isolate) from the soil (i.e. reducing the soil to tree hydraulic conductance) and (ii) limit its water losses during drought. Pioneering work on this topic was conducted by Nobel and Sanderson (1984) who showed that roots of desert succulent plants could act as "rectifier," thereby being able to absorb water in wet soil, but to limit desiccation in dry soils, which seems consistent with our results.

We used the SurEau model to evaluate whether root hydraulic isolation from the soil could explain the observed water potential patterns in *P. halepensis* in mixture, consistently with Nobel and Sanderson's (1984) work. We implemented a decrease in root hydraulic conductance (K_{root}) as the plant water potential decreases. Simulation results indicated that reducing only K_{root} alone did not allow to simulate higher Ψ_{pd} than Ψ_{soil} for *P. halepensis* (Fig. 5A). This means that the water losses that occurred after stomatal closure—which resulted from the leaf cuticular conductance (g_{cuti}), set in the model using the average value measured for *P. halepensis*, were high enough to cause plant water potential to drop even after a strong decrease in K_{root} isolating the plant from the soil. We thus implemented in the model a downregulation of the leaf cuticular conductance (g_{cuti}) with decreasing tree RWC, which is in line with empirical data obtained for this species using the DroughtBox methods (Billon et al. 2020; Supplementary Fig. S6B). Simulations showed that, although the reduction of g_{cuti} alone attenuated the decrease in plant water potentials, the tree kept dehydrating along with the soil water potential drop triggered by *Q. ilex* transpiration. In a last sensitivity test, we implemented a decrease of both K_{root} and g_{cuti} under drought, which caused *P. halepensis* water potentials to depart from soil water potentials (Fig. 5A), in line with our observations. This suggests that these 2 mechanisms jointly could allow *P. halepensis* to prevent dehydration under drought. In a natural forest context, tree isolation from the soil during drought has already been proposed to explain the cooccurrence of isohydric and anisohydric trees (Pangle et al. 2012; Plaut et al. 2012; Aguadé et al. 2015; Moreno et al. 2021). The mechanisms for such an isolation are of several types, including the formation of cortical lacunae under fine roots (Cuneo et al. 2016; Duddek et al. 2022), which reduces the water transfer to the root stele and hence affects the root hydraulic conductance. Root shrinkage might also explain the plant–soil hydraulic disconnection by creating gaps between soil and fine roots, interrupting the hydraulic conductance between both of them. Furthermore, the inhibition of the synthesis of proteins such as aquaporins facilitating the water transport in the transcellular pathway (Domec et al. 2021) or even fine root mortality (Leonova et al. 2022) could also lead to hydraulic isolation. Yet, to our knowledge, the mechanisms leading to strong plant hydraulic isolation from both the soil and the atmosphere had never been proposed until now.

Table 3. *F* statistics and *P* values of factors in the ANOVA of the predawn water potentials of *Q. ilex* (Ψ_{pd} QI) in mixtures according to predawn water potentials of *P. halepensis* (Ψ_{pd} PH) and root separation modality (with or without root separation; Ψ_{pd} QI~ PH*Separation modality)

Factors	F_value	P_value
Ψ_{pd} PH	338.1	$<2.2e^{-16}$
Separation modality	10.9	0.002
Ψ_{pd} PH: separation modality	5.14	0.03

Table 4. Species-specific parameters used in the model to describe the water use and drought tolerance strategies of the species

Traits (symbol, units)	*P. halepensis*	*Q. ilex*	Comments	References
Water potential causing 10% stomatal closure (Ψgs_10, MPa)	−1.5	−1	None	Martin-StPaul et al. (2017)
Water potential causing 90% stomatal closure (Ψgs_90, MPa)	−2.5	−4	None	Martin-StPaul et al. (2017)
P50 of the xylem of the vulnerability curve (MPa)	−4.7	−7.1	Constant for all apoplasmic organs	Sergent et al. (2020); Martin-StPaul et al. (2017)
Slope of the xylem vulnerability curve (%/MPa)	78	23	Constant for all apoplasmic organs	Sergent et al (2020); Martin-StPaul et al (2017)
Osmotic potential at full turgor (π100, MPa)	−1.26	−1.9	Constant for all symplasmic organs	Martin-StPaul et al (2017); Moreno (2022)
Modulus of elasticity of the symplasm (ϵ, MPa)	9.7	16	Constant for all symplasmic organs	Martin-StPaul et al (2017); Moreno (2022)
g_{cuti_ref} (mmol m^{-2} s^{-1})	1.1	2.38	Targeted for a sensitivity analysis	Billon et al (2020); Moreno (2022)
Leaf area (m^2)	0.17	0.14	Constant	This study
Succulence (gH_2O m^{-2})	300	145	None	Ruffault and Martin-StPaul (2024)
K_{plant} (Leaf_specific, mmol m^{-2} s^{-1} MPa^1)	0.8	1.4	None	This study

Table 5. Soil parameters (Puéchabon site) describing the water retention curves and the changes in soil conductivity, used for all 3 soil layers in SurEau simulations

θ_{sat}	θ_r	α	n	K_sat (mol s^{-1} MPa^{-1})
0.28	0.1	0.0005	2	5

The anisohydric *Q. ilex* could increase root hydraulic conductance to the soil in the mixture through increased root length

Q. ilex in "true mixture" (i.e. pots without root separation) had lower water stress for a given level of soil drought (i.e. higher predawn water potential for a given soil water potential, Fig. 3A). This suggests that this species is able to increase soil water use when grown in association with *P. halepensis*. Different hypotheses could explain this phenomenon. It could be argued that differences between Ψ_{pd} and Ψ_{soil} reflect shifts in the root profiles in mixtures compared to monocultures as proposed by Bello et al. (2019). Indeed, if roots explored only a part of the available soil, Ψ_{pd} would equilibrate with this soil subspace, possibly differing from the overall Ψ_{soil} measured at the plot level. However, such an effect should be minimal in our study for 2 reasons. Firstly, we used on purposes very small pots (12 L) to maximize the occupation of the soil volume by tree roots, which was verified when the plants were uprooted at the end of the experiment, thus making this assumption unlikely. Secondly, the measurements of soil resistivity made at 2 different depths showed no significant differences between the 2 measured depth levels (1/3 and 2/3 of the pot height), for none of the modalities (Supplementary Fig. S2, $P > 0.05$). Because resistivity varies according to a power law as a function of water content (Archie 1942; Waxman and Smits 1968), which means that when the soil is dry, little variation of soil water content translates into a large change in resistivity, our measurements indicate that there is most likely no spatial segregation in the uptake of soil water by roots. Alternatively, one can postulate that differences between Ψ_{pd} and Ψ_{soil} resulted from changes in the soil hydraulic conductance, which could occur as a result of increase fine root density. We carried out simulations with SurEau to test this hypothesis (Fig. 5B). Hence, we conducted simulations in which we assumed that the increase in soil conductance might be achieved through an increase in the exchange surface between soil and roots ("single root" approach, see the Materials and methods section). We tested this hypothesis by varying the fine root length per unit soil volume. This sensitivity test showed that changing K_{soil} can change the Ψ_{pd} vs. Ψ_{soil} relationship (Fig. 5B). Indeed, reducing the value of this parameter (graph "root length × 1/2," Fig. 5B) resulted in a departure between Ψ_{pd} and Ψ_{soil} as observed in the monoculture, whereas increasing root length resulted in Ψ_{pd} and Ψ_{soil} being comparable, as observed in the mixture without root separation. Interestingly, some studies have already reported modifications toward higher fine root density in mixture conditions (Sun et al. 2017; Wambsganss et al. 2021), identifying this phenomenon as a complementarity effect between associated species.

Ecological and practical implications

Our study has different larger scale implications for forest management and vegetation modeling. First of all, it is noteworthy that the positive effect of mixture—particularly highlighted for *Q. ilex*—was not found in the pots designed to separate the root systems of the 2 species with a mesh (Figs. 2 and 3, Supplementary Fig. S3). This indicates that root systems of the 2 individuals must be entangled for the mixture effect to be efficient. This result is important for tree plantation as it supports the premise that intimate species mixture is required to observe a mixture effect in diverse forests. Overall, this is in line with the growing body of evidence showing the importance of tree–tree interactions in driving the biodiversity vs. ecosystem functioning relationships (Trogisch et al. 2021).

In addition, our study could explain how mixing tree species with contrasting hydraulic strategies limited the hydraulic risk during extreme drought by using a mechanistic model. This paves the way for developing numerical tools allowing to explore how to design species mixture resilient to climate change. Although the mechanisms highlighted remain to be tested at larger scale, they could change our representation of the mechanisms that determine water stress in plant communities. Although positive effects of mixtures can come from a complementarity of water use linked to spatial segregation of root systems or different water uptake depth as usually proposed (Bello et al. 2019; Grossiord et al. 2019; Haberstroh and Werner 2022; Liu et al. 2023), we provided support that other mechanisms can be involved. Indeed, differences in water use regulation strategies of species along with modifications of hydraulic connections between the plant and the soil can alone explain the observed behaviors in a model. This challenges the way vegetation models represent water stress in plant communities. To date, the majority of process-based models assume that soil water deficit in the rooting zone drives the water status of the plant. However, we provide evidence that changes in the hydraulic connection from the soil can make the plant, in dry conditions, behave independently from the soil water status. Implementing such processes in larger scale vegetation models could help to refine and better predict species interactions and drought-induced effects on forest communities. This would represent a step forward in the development of tools allowing to design drought resilient mixtures.

Materials and methods

Seedlings and experimental design

Our study focused on 2 tree species commonly found in the Mediterranean region and naturally co-occurring over large areas: the isohydric Aleppo pine (*P. halepensis*, drought avoidant with tight water loss control) and the anisohydric holm oak (*Q. ilex*, drought tolerant with more progressive water loss control). The experiment compared water status and hydraulic traits during drought among seedlings grown in mixture and monocultures, and with or without physical barrier preventing intimate root contact among the 2 plants (see below). This latter treatment aimed at testing whether the root systems of the 2 species need to be entangled to observe mixture effects, or if soil matrix potential gradients are large enough to trigger mixture effect without a close contact between root systems.

From 2019 to June 2021, saplings were grown at the French National Forestry Office of France (ONF) nursery in Cadarache (southeast of France) and were watered twice a week to field capacity and fertilized once a week. Seedlings of *P. halepensis* and *Q. ilex* (1 and 2 yr old, respectively) of equivalent dimensions were repotted in January 2020. Ninety trees of each species were planted in 12-L containers, each containing 2 individuals per pot, either in monoculture or in mixtures. The soil was composed mainly of organic matter and of sand (~20%). Half of the pots were equipped with a physical barrier made of acrylic fabric with a 30-μm mesh that precluded root colonization from one side to the other of the pot but allowed water transfer between the 2

separated compartments. One month before the start of the experiment (June 2021), pots were brought on the campus of INRAE in Avignon (Southeast France) to acclimate in the experimental greenhouse. The greenhouse was equipped with air temperature, humidity (HD 9817T1), and radiation loggers. It included an independent regulation of climate through aeration (window opening or forced ventilation) and cooling (humidification of the air entering through a "cool box"). These systems allowed regulating the environment of the greenhouse according to the defined settings. In addition, the sidewalls of the greenhouse had been whitewashed to homogenize the radiation and the temperature. The temperature was kept between 25 and 35°C, relative humidity (RH) between 40% and 75%, and maximum diurnal photosynthetically active radiation (PPFD) below 1,000 μmol m^{-2} s^{-1} (Supplementary Fig. S1).

During the acclimation period in the greenhouse, watering was applied as in the nursery. Among the initial batch of 90 pots, we selected 54 pots for which the 2 trees were alive and had reached a height between 40 and 60 cm with less than 10 cm height differences between the 2 trees. Pots were divided into 2 batches: a batch of 6 pots per composition (36 pots in total) that was assigned to the drought experiment and a batch of 3 pots per treatment (18 pots in total) that was assigned to a control treatment in which trees were maintained watered all along the season (2 times a week). The day before the beginning of the experiment, at the end of the afternoon, all pots were watered at saturation and weighted.

The experiment was set up during the summer of 2021. It consisted in applying a drought treatment (watering stop) to potted *P. halepensis* and *Q. ilex* trees grown in monoculture or in mixture while monitoring ecophysiological variables at 5 different dates. All pots were monitored once a week, from July 26 to August 18, for leaf water potentials, leaf gas exchanges, and pot weights.

Plant water potential measurements

Water potentials were measured at predawn once a week across the experimental period for all trees monitored. The evening before measurements, 1 leaf (*Q. ilex*) or small twig (*P. halepensis*) of each tree was covered with an aluminum foil and placed in a ziplock plastic bag. In addition, to limit tree nocturnal transpiration and allow water potential equilibration between the tree and the soil (Rodriguez-Dominguez et al. 2022), trees were covered with a plastic bag and a piece of wet paper was included under the plastic bag. Samples were collected before sunrise, between 4 and 5 AM, kept into the ziplock, and immediately placed in a cooler for water potential measurement. The 108 measurements were done randomly in less than 4 h following sampling, with a Scholander pressure chamber (PMS model 1505D).

Tree leaf gas exchanges

Leaf level gas exchanges were measured using 2 portable photosynthesis system (LI-6400XT) for all trees at all dates except the second one due to a breakdown of the greenhouse system affecting cooling system. Measurements were done between 11 AM and 3 PM, period during which photosynthetic active radiation (PAR) in the greenhouse was highest and stable (between 600 and 1,000 μmol m^{-2} s^{-1}). Licor chamber conditions were set to keep close to the greenhouse while providing nonlimiting conditions: PAR was set at 1,000 μmol m^{-2} s^{-1}, the block temperature was set at 25°C, and flow rate and scrubbing were adjusted to maintain RH between 60% and 80%. The leaves were allowed to acclimate for at least 3 min in the chamber before measurement to ensure gas exchange stability. For each leaf (*Q. ilex*) or needle bunch (*P. halepensis*), 10 values were recorded during 1 min and the average was used in the data analysis. After the measurement, the areas of leaves or needles included in the chamber were cut and stored in a plastic bag inside a cooler. The day after, leaf area was measured to correct gas exchange computation with actual leaf area in the chamber. Samples were then dried during 48 h at 70°C to estimate specific leaf area.

Tree biomass and leaf area estimates

We estimated leaf area of each tree at the beginning and the end of the experiment using a method relying on profile photographs, adapted from Ter-Mikaelian and Parker (2000). It is based on a calibrated relationship between the projected area of the tree profile and the foliage biomass estimated destructively. For each species, we first built a calibration relationship between the number of tree pixels in profile photographs and the foliage biomass. For the calibration relationship, trees were selected to span the range of sizes encountered in the experiment. We sampled trees before the beginning of the drought experiment (June 2021), but also after the experiment (September 2021), to account for potential changes in size or leaf area or angulation that could have occurred during the summer and influenced the relationship. For each tree, the profile surface projected area was estimated by photography. All the settings were made to ensure a constant reproduction ratio (i.e. constant dimensions of real object dimensions per pixel) among photographs. To obtain foliage dry mass, all trees used for this calibration were cut at the base of the stem after taking the photographs. Tree parts were sorted to separate green foliage, dead foliage, and the rest, which was almost entirely made of stems. Tree parts were then dried at 70°C for 3 d (leaves/needles) or until there was no variation in dry mass (almost 1 wk). The leaf area of each tree was computed by converting foliage dry mass into area using specific leaf areas estimated on leaf gas exchange measurement samples.

At the end of the experiment and for droughted pots, the belowground part of each tree was uprooted. The rooting system was washed to separate the soil particles from the roots. Each plant was hung vertically, and the rooting system extension (maximal length and width) was measured using a ruler, with a millimeter resolution. The root system was then dried out at 70°C in an oven for at least 10 d, until there are no more weight variations, and the total dry mass was estimated.

Soil water content and soil water potentials

Pots were weighted at each measurement dates in the morning (ca. 8 AM) and at the end of the measurement day (ca. 5 PM). Soil water content was estimated at the pot level, by subtracting the total pot weight (measured in the morning) by the soil dry mass and the total fresh tree biomass. Soil water potential (Ψ_{soil}) was then estimated at the pot level from the normalized soil water content of the pots and water retention curves determined in the laboratory on soil samples ($V = 6$ cm^3). The determination of the retention curve was made with the combination of suction table ($\Psi_{soil} > -0.01$ MPa), pressure plate ($\Psi_{soil} > -1.5$ MPa), and dew point hygrometer (WP4C, Decagon—$\Psi_{soil} < -1.5$ MPa) methods (Dane and Topp 2020). Five soil sample replicates were used for each point of the retention curve, and the gravimetric water content was determined from fresh and dry weight obtained after drying in an oven at 70°C (temperature limit to avoid organic matter degradation) for about 1 wk. To perfectly match the data, 2 different retention curves using van Genuchten relationships (van

Genuchten 1980) were fitted. A first retention curve was fitted with gravimetric water contents above 0.1214 g g^{-1} (corresponding to $\Psi_{soil} = -1.25$ MPa). For gravimetric water content lower than 0.1214 g g^{-1}, a second of retention curve was fitted. The retention curves take the following form:

$$\psi_{soil} = \frac{\left(\left(\frac{1}{\Theta}\right)^{\frac{1}{m}} - 1\right)^{\frac{1}{n}}}{\alpha}, \quad (1)$$

where m, n, and α are empirical parameters describing the typical sigmoidal shape of the function and Θ is the normalized water content. Water potentials were calculated from this fit using the gravimetric water contents of pots estimated at each measurement date. The parameters of the curves are provided in Supplementary Fig. S8 and Table S4.

The normalized water content (Θ) was computed for each pot as follows:

$$\Theta = \frac{W - Wr}{Wsat - Wr}, \quad (2)$$

with W the gravimetric water content of the pot at a given time, Wr the residual gravimetric water content, and Wsat the gravimetric water content at saturation. It was measured at the end of the experiment after drying the soil at 70°C. Wsat was estimated from the first weight measurement of the experiment, after the pots were irrigated at saturation. W and Wsat were computed by removing the mass of the tree and the pot to the total weight measured during the experiment. The total tree weight was measured at the end of the experiment, by assuming that tree growth that could have occurred during the experiment can be neglected due to the extreme drought experienced by the tree.

Since soil water potentials were not directly measured, we calculated soil water potentials from water contents as described above and also plus or minus the largest error possible combining both the retention curve precision and the weighting uncertainty (Supplementary Fig. S4). The largest difference between measurements and the fitted van Genuchten curves in the [−6, 0] MPa range (a range consistent with our experiment) was 0.63 MPa. The scale used to weight the pots had a measurement precision of ±0.5 g. We then compared tree water potentials to the 3 estimates of soil water potentials (Supplementary Fig. S4).

Soil resistivity measurement

Electrical resistivity of soil in pots was measured using electrical resistivity tomography (ERT). Four pots (including 1 control) per modality (monoculture or mixture, with or without root separation system) were selected. On these pots, electrical resistivity was monitored with time over 2 radial planes, located at 1/3 and 2/3 of the pots' height, by inserting 20 stainless steel screws (2 cm long) equally spaced (3.9 cm) along the column's circumference. ERT measurements were done using an ABEM SAS 4000 resistivity meter connected to all these electrodes. All quadrupole combinations were used, including reciprocal measurements for assessing error and measurement quality. The resistivity measurements were taken before the start of the experiment (when the pot substrates were at field capacity), in the middle, and at the end of the experiment. In the late dry situations, it was necessary to add a small amount of water at electrodes to enable soil–electrode electrical contact and resistivity measurements. Soil resistivity distribution at the 2 heights was obtained from the inversion of apparent resistivity using ResIPy software (Blanchy et al. 2020).

Statistics

We evaluated the effect of species and measurement date and their interactions on the water potential of trees by using a linear mixed model. Then, for each species independently and root separation modalities (root separation or not), we assessed the effect of pot composition (mixture or monoculture association) on predawn water potentials by considering date, composition, and their interaction as explanatory factors. As we did not find any significant differences between water potentials of monoculture with and without root separation for each species (Supplementary Fig. S9), we decided to pool them for the analysis. We also tested the differences between soil and tree water potentials at each measurement date using Student's t tests. Finally, we applied post hoc Tukey HSD tests to evaluate differences between pot modalities (composition and root separation) for gas exchange variables (leaf conductance and transpiration, Supplementary Fig. S3). All statistical analyses were performed with the R software (3.5.2, R Development Core Team 2018) with the packages lme4 and agricolae (Bates et al. 2015; de Mendiburu 2023).

Model analysis using SurEau

General overview of the model

We performed sensitivity analysis with a soil–plant hydraulic model in order to explore the mechanisms driving the mixture effects during an extreme drought. We used the SurEau model coded in C, which has been extensively presented previously (Cochard et al. 2021). In brief, SurEau has been designed to model extreme drought and accounts for the processes occurring after the point of stomatal closure (i.e. cuticular water losses as well as losses of hydraulic conductance and plant water stocks due to xylem embolism). It computes water fluxes along a discretized soil–tree atmosphere continuum and accounts for variations of plant and soil water stocks and water potential (which are the state variables of the model) by using diffusion laws (conductance and water potential gradients between compartments) and capacitances. The model is driven by hourly climate data (temperature, VPD, radiation, and wind speed), which are downscaled at smaller time step to perform computation. At each time step, the model starts with the computation of leaf stomatal and cuticular transpiration as the product between leaf-to-air vapor pressure deficit and stomatal and cuticular conductance. These fluxes are used to trigger a drop in water content in the leaves, which is translated into a water potential drop (using the specific capacitances). In turn, leaf water potential is used to compute water flows with the adjacent compartments and update their water potential and water quantities. This approach is applied to all compartments (including the soil) over 1 small time step to avoid numerical instabilities (ca. 0.01 s; Ruffault et al. 2022) and repeated until the plants eventually reach total hydraulic failure (loss of xylem conductance) in all apoplasmic compartments.

Stomatal conductance (gs) was modeled using a Jarvis formulation, by which gs depends on radiation and leaf water potential (Cochard et al. 2021). The leaf stomatal response to water potential was set species specific as in Martin-StPaul et al. (2017). The leaf cuticular transpiration is modeled as a result of the product between vapor pressure deficit and leaf cuticular conductance (g_{cuti}, which by default was set constant for each species).

The soil is discretized into 3 soil layers and the plant system into 4 organs (roots, trunk, branches, and leaves). Each plant organ is composed of an apoplasmic (i.e. xylem) and a symplasmic compartment, each being defined by a capacitance and conductance with the surrounding compartments. The capacitance of

the symplasm depends on the water potential according to the pressure volume curves, whereas the capacitance of the apoplasm is set constant (Martin-StPaul et al. 2017; Cochard et al. 2021). The organs are connected between each other axially via their apoplasm, and each organ's apoplasm is connected radially with a symplasm. The hydraulic conductance of the xylem (apoplasm can decline as a result of xylem embolism. Xylem embolism is computed by using the xylem vulnerability curve to cavitation. Each soil layer is connected to a root in series, and all roots are connected to the trunk in parallel. The soil hydraulic conductivity and the soil water potential of each layer are computed as a function of soil water quantity and the saturated conductivity using the van Genuchten model (van Genuchten 1980). The hydraulic conductance between the soil and the fine roots for each soil layer is computed by using the soil conductivity and the scaling factor (B_{GC}) based on fine root density proposed by Gardner–Mualem, as described in Martin-StPaul et al. (2017):

$$k_{soil} = B_{GC}.K_{sat}.\mathrm{REW} \times \left[1 - \left(1 - \mathrm{REW}^{\frac{1}{m}}\right)^{m}\right]^{2}, \quad (3)$$

with K_{sat} the soil hydraulic conductivity at saturation, m a parameter from the van Genuchten soil water retention curve, REW the RWC ($\mathrm{REW} = \frac{\theta - \theta_r}{\theta_s - \theta_r}$, with θ the actual soil water content, θ_r the residual soil water content, and θ_s the soil water content at saturation), and B_{GC} the scaling factor calculated as follows:

$$B_{GC} = \frac{2\pi.\mathrm{La}}{\ln\left(\frac{1}{r\sqrt{\pi}.\mathrm{Lv}}\right)}, \quad (4)$$

with L_a and L_v the root length per soil area and volume and r the radius of fine roots. The root length was the target of sensitivity analysis (see below sensitivity analysis).

Each fine root is connected to the soil layer through a symplasmic conductance, which is set constant by default (K_{root}). This root symplasmic conductance has been modified in the sensitivity analysis to test the effect of plant isolation from the soil during drought (see below sensitivity analysis).

In the present study, the model was improved to include the possibility for 2 trees to absorb water in the same soil volume. In principle, 2 codes corresponding to 2 trees, parameterized for monoculture of *P. halepensis*, monoculture of *Q. ilex*, or for mixture, were run in parallel.

General considerations about the model parameterization and application

We describe below the main parameters used in this study and refer the reader to Cochard et al (2021) for further information about parameters' definitions and their implementations. The parameters can be separated into 3 types:

1. Plant size-related traits including (i) the hydraulic conductance for the different plant compartments, (ii) the water volumes of the different compartments, and (iii) the overall leaf area and fine root length and area. These parameters can be derived from direct measurements and from allometric relationships.
2. Physiological traits including (i) the pressure volume curve parameters (π100, ϵ), (ii) the vulnerability curve to cavitation (P50, slope), (iii) the stomatal response to radiation and to water potential, and (iv) the leaf cuticular conductance.
3. Soil parameters including the soil depth and the water retention curve parameters (van Genuchten equation parameters) for each soil layer.

In the simulations made for this study, size-related parameters were set constant for the 2 species. We assumed each plant to be small plant of 1 m of height with a stem diameter of 1 cm and a leaf area 0.2 m^2. The volumes of water of the different woody compartments (branches, trunk, and leaves) were computed assuming a branch to trunk ratio of 0.5 and a root to shoot ratio of 0.3. The volumes of water in the leaves were computed based on the leaf area and a succulence of 100 g/m^2. The default fine root area was set equal to the leaf area (assuming a fine root to leaf area ratio of 1). The fine root length was computed assuming a fine root diameter of 0.5 mm and distributed equally among the 3 soil layers.

The hydraulic conductance of the different compartments was defined by using a total leaf-specific hydraulic conductance around 1 mmol m^{-2} s^{-1} MPa^{-1} (value for small trees consistent with our measurements and with the previous literature; Mencuccini 2003), which was distributed among the plant compartments assuming a typical hydraulic architecture (Tyree and Ewers 1991; Cruiziat et al. 2002). The hydraulic resistance was thus distributed as follows: 20% in the leaf symplasm, 20% in the leaf apoplasm, 8% in the branch apoplasm, 2% in the stem apoplasm, 10% in the root apoplasm, and 40% in the root symplasm. The radial symplasmic resistance was computed for each woody compartment (roots, trunk, and branch) using the developed areas and a symplasmic conductivity of 1 (mmol m^{-2} s^{-1} MPa^{-1}) for trunk and branches and 3.5 (mmol m^{-2} s^{-1} MPa^{-1}) for roots (Cochard et al. 2021). Note that the root symplasmic hydraulic conductance (K_{root}) dictates the water fluxes between the soil and the inner part of the root was the target of sensitivity analysis (see below).

The physiological traits used in the model to define the water use and drought resistance strategies of the 2 studied species were set by using previously published literature or personal data (Table 4). For the sake of simplicity, potential segmentation of xylem vulnerability was omitted and the same vulnerability curve to cavitation was used for all compartments of the same species. Similarly, the same species-specific leaf PV curve was used to compute the symplasmic capacitance of all the symplasmic compartments. The stomata response to leaf symplasmic water potential used in the model for water loss regulation was set by using published data of concurrent measurements of stomatal conductance and leaf water potential (Klein 2014; Martin-StPaul et al. 2017). The maximum stomatal conductance and the stomata response to incident PAR were set constant among species as in Ruffault et al. (2022). The leaf cuticular conductance was taken from Billon et al. (2020). It is based on measurement of leaf water loss under controlled climatic conditions, averaged after the point of stomatal closure. This value has also been the target of a sensitivity analysis (see below).

Since not all the parameters of the specific soil used in the experiment have been measured, the soil hydraulic parameters (Table 5) were taken from a typical French Mediterranean site where the SurEau model was previously applied (Ruffault et al. 2023). However, to generalize our results, a sensitivity analysis was made for a large range of soils using parameters from Carsel and Parrish (1988) (Supplementary Fig. S10 and Table S5). For each simulation (in monoculture and mixture with the different soil parameters), we used the THF computed by the model as an indicator of drought stress resistance. THF corresponds to the

modeling time required for the plant to reach water potential causing 100% loss of hydraulic conductivity. For each type of soil and each species, we computed the relative THF in mixture compared to monoculture as THFrelative = THFmixtures/THF monoculture. A value of 1 means that mixture and monoculture experienced the same water stress. The results (Supplementary Fig. S10) highlight an overall consistent pattern (regardless of the soil type) with our current results: in mixture, hydraulic risk (i.e. THF) increases for *Q. ilex* and decreased for *P. halepensis*.

The model was initialized with a soil at the field capacity. Then, the model was forced with constant climatic conditions from day to day, but variable diurnally as in Cochard et al. (2021) and Ruffault et al. (2022). The rainfall was set to 0 to explore a desiccation dynamic as in the experiment. Simulations were stopped when the 2 plants reached total hydraulic failure (defined as 100% loss of conductivity in the stem). The time to reach hydraulic failure (THF) was used as an index of drought stress resistance to compare the species and treatments (mixture and monocultures).

Hypothesis testing using SurEau model sensitivity analysis

1. Benchmark simulations

To test the hypotheses presented in the introduction (illustrated in Fig. 1B), we first performed *benchmark* simulations. Simulations with 2 individuals in monoculture or mixture competing for the same amount of water were performed using the default parameters described in the section above (Table 4). The results obtained with these simulations were in accordance with the hypothesis drawn in Fig. 1B but departed from the empirical results. Indeed, these simulations were unable to reproduce the relatively constant water potential of the isohydric *P. halepensis* species during extreme drought. As explained above, the patterns of Fig. 1B hold only under the assumptions that (i) there is no significant segregation in soil exploration by the 2 species (which is reasonably the case of our experiment as we observed that root systems of the 2 species colonized the full soil volume, which was set low on purpose) and (ii) that the 2 individuals are highly connected to the soil (i.e. large hydraulic conductance between the soil and the fine roots).

Consequently, we performed different types of sensitivity analysis with SurEau in order to explore how changes in soil or root hydraulic conductance could help to represent the observed empirical patterns. The water flow between the soil and inner part of the root being modeled using 2 different conductances (K_{soil} and K_{root}, see above), and these 2 conductances were modulated as described below.

2. Testing the "isolation effect" for *P. halepensis*: can we explain the relatively constant water potential of *P. halepensis* with variable root hydraulic conductance (K_{root}) and cuticular conductance (g_{cuti})?

For *P. halepensis*, empirical data support that plant water potential can be higher than soil water potential during extreme drought, suggesting that this species can behave independently from the soil and maintain its water potential constant even if soil water potential decreases. Previous studies suggested that decline in conductance between the soil and root can occur during drought (North and Nobel 1997; Cuneo et al. 2016; Duddek et al. 2022). This can be represented in the model by decreasing the root symplasmic conductivity when root water potential decreases. Therefore, we implemented a variable K_{root} by assuming a variable gap fraction in the root cortex:

$$K_{root} = \frac{K_{root_{symp0}} * (100 - Cortex_{Gap})}{100}, \quad (5)$$

with $K_{root_{symp0}}$ the initial hydraulic symplasmic conductivity and $Cortex_{Gap}$ the proportion of gap in the root cortex, which we computed by assuming a sigmoidal dependence to the root symplasmic water potential $P_{rootsymp}$:

$$Cortex_{Gap} = \frac{100}{(1 + \exp(K_{varP2}/25 * (P_{rootsymp} - K_{varP1})))}, \quad (6)$$

with K_{varP1} the water potential causing 50% of cortex gap and K_{varP2} the slope at the point of inflexion of the sigmoid (Supplementary Fig. S5).

We used this implementation to perform simulation in mixture conditions, still parameterizing *Q. ilex* as in benchmark conditions. Such implementation led to an acceleration of hydraulic failure for *P. halepensis*, which is explained by the fact that there is less water supply from the soil, but still significant cuticular losses that are not anymore be compensated, and thus lead to an excessive plant desiccation. We therefore also tested whether accounting for a concurrent decrease in leaf cuticular conductance during drought stress, a phenomenon already observed on cut branches of *P. halepensis*, could explain—alone or in combination with the reduction in root conductance—the observed pattern (Supplementary Fig. S6A). To do so, we implemented a linear decrease of the cuticular conductance (g_{cuti}) with the leaf symplasmic RWC (Supplementary Fig. S6B) as observed for *P. halepensis* using a DroughtBox (Billon et al. 2020). We assumed that after turgor loss point, g_{cuti} decreased linearly:

$$\text{if}(RWC_{leaf} < RWC_{tlp}),$$

$$g_{cuti} = g_{cuti_{ref}} * (1 - (RWC_{tlp} - RWC_{leaf}) * RWC_{sens}), \quad (7)$$

$$\text{else } g_{cuti} = g_{cuti_{ref}},$$

with RWC_{leaf} the leaf symplasmic RWC, RWC_{tlp} the leaf RWC at turgor loss point, RWC_{sens} the sensitivity of g_{cuti} to RWC, and $g_{cuti_{ref}}$ the reference leaf cuticular conductance. We found that combining both, a reduction of K_{root} and a reduction of $g_{cuti_{ref}}$, led to patterns of water potential consistent with our empirical findings.

3. Testing the potential increase of soil hydraulic conductance through increased root length for *Q. ilex* in mixture

Secondly, for *Q. ilex*, we noticed a lower water stress under mixture, which was also linked to a change in the relationship of the soil water potential (Ψ_{soil}) vs. plant predawn water potential (Ψ_{pd}). Higher plant water potential for a given soil water potential was found under mixture compared to monoculture. Such pattern could be explained by an increase of the soil hydraulic conductance that, as evidenced by Equations 3 and 4, can be related to the density of fine roots (L_a and L_v, the length of fine roots per m^2/m^3 of soil). It is also consistent with the observed increase in root length under mixture conditions (Supplementary Fig. S7). We therefore performed a sensitivity analysis to the density of fine roots under monoculture conditions to test whether these trait changes explain the observed mixture effect on water status.

Acknowledgments

We would like to thank the ONF-PNRGF (Pôle National des Ressources Génétiques Forestières de l'Office National des Forêts) nursery of Cadarache (13) for caring for the plants 2 yr prior to the experiment. Thanks also to Gilles Vercambre and the greenhouse staff of the PSH unit for accompanying us during the experiment. Finally, thanks to the URFM and EMMAH INRAE staff, in particular to Henri Picot, Denis Portier, Arnaud Jouineau, Marion Parizat, Didier Besombes, Didier Betored, Philippe Petit, Arnaud Chapelet, and to Anouk Brisset and Léo Corridor (students), for their help in the setting up of the experiment and acquiring data.

Author contributions

M.M., N.K.M.-S., and H.C. designed the research. F.J. and O.M. helped in the setting up of the experiment. In particular, F.J. coordinated the cooperation with the ONF-PNRGF (Pôle National des Ressources Génétiques Forestières de l'Office National des Forêts) nursery of Cadarache (13) and secured a site in the greenhouse. O.M. controlled and installed devices used for the measurements. M.M. and N.K.M.-S. performed research with the help of C.D., R.D., G.S. and P.F.-C. H.C. and N.K.M.-S. performed the model simulations. M.M. analyzed the data with the help of N.K.M.-S., G.S., C.D. and H.C. M.M. write the first draft of the manuscript, which was then modified by both N.K.M.-S. and M.M. All authors contributed to the review of the manuscript and approved the final version.

Supplementary data

The following materials are available in the online version of this article.

Supplementary Figure S1. Meteorological variables recorded in the greenhouse during the experimentation: RH, PAR, and temperature, and soil water potentials of droughted pots.

Supplementary Figure S2. Mean resistivity of the top and bottom profiles of pots (1/3 and 2/3 of the height of a given pot) at the end of the experiment according to pot modality.

Supplementary Figure S3. Dynamics of leaf transpiration and conductance for *Q. ilex* (QI) and *P. halepensis* (PH), either in monocultures (black dots) or mixtures (gray dots), without (left panel) or with (right panel) root separation.

Supplementary Figure S4. Impact of soil water potential computation uncertainty on the difference between soil and tree water potentials.

Supplementary Figure S5. Relationship between root hydraulic conductance (K_{root}) and root symplasmic water potential implemented in the SurEau model simulations to test the hypothesis of soil to root isolation for *P. halepensis*.

Supplementary Figure S6. Relationship between the leaf cuticular conductance (g_{cuti}) and the leaf RWC used to test the hypothesis of leaf to air isolation for *P. halepensis*.

Supplementary Figure S7. Average root length of *Q. ilex* (gray bars) and *P. halepensis* (white bars) for the different pot composition modalities.

Supplementary Figure S8. Soil water retention curves obtained on subsamples of soil and used to extrapolate soil water potential (or soil matric potential, h) of the pots.

Supplementary Figure S9. Averages and SD of plant predawn water potentials (Ψ_{pd}) in monocultures.

Supplementary Figure S10. Time of Hydraulic Failure (THF) of both species relative to monoculture (relative THF = THFmixture/THFmonoculture, a value of 1—shown by the dashed red line—indicates that mixture and monoculture experience the same water stress) in the soil type given by Carsel and Parrish (1988) and for the Puéchabon soil used for simulation.

Supplementary Table S1. ANOVA of the mixed model for tree predawn water potential to test date and species effect.

Supplementary Table S2. ANOVA of the mixed models to test the composition effect (monoculture vs. mixture), per species and type of pot (with or without root separation), for tree water potential (measured at predawn).

Supplementary Table S3. Water flux estimate between the compartment of the pots at the penultimate and last dates of measurement.

Supplementary Table S4. Parameters of the retention curve for the first ($\Psi_{soil} < 12.5$ bars) and second ($\Psi_{soil} > 12.5$ bars) fits of the van Genuchten equation.

Supplementary Table S5. Soil parameters describing the water retention curves according to soil types given by Carsel and Parrish (1988).

Supplementary Method S1. Computation of water fluxes between the 2 pot compartments of the mixture with root separation modality.

Funding

M.M. was supported by the French Environment and Energy Management Agency (ADEME) in the form of a PhD scholarship. The experiment was funded by Agence Nationale de la Recherche (MixForChange, ANR-20-EBI5-0003; TAW-tree, ANR-23-CE01-0008-01) and the Metaprogramme ACCAF Drought&Fire.

Conflict of interest statement. None declared.

Data availability

All data are incorporated into the article and its online supplementary material.

References

Adams HD, Zeppel MJB, Anderegg WRL, Hartmann H, Landhäusser SM, Tissue DT, Huxman TE, Hudson PJ, Franz TE, Allen CD, *et al.* A multi-species synthesis of physiological mechanisms in drought-induced tree mortality. *Nat Ecol Evol*. 2017:1(9):1285–1291. https://doi.org/10.1038/s41559-017-0248-x

Aguadé D, Poyatos R, Rosas T, Martínez-Vilalta J. Comparative drought responses of *Quercus ilex* L. and Pinus sylvestris L. in a montane forest undergoing a vegetation shift. *Forests* 2015:6(12):2505–2529. https://doi.org/10.3390/f6082505

Allen CD, Macalady AK, Chenchouni H, Bachelet D, McDowell N, Vennetier M, Kitzberger T, Rigling A, Breshears DD, Hogg EH, *et al.* A global overview of drought and heat-induced tree mortality reveals emerging climate change risks for forests. *For Ecol Manag*. 2010:259:660–684. https://doi.org/10.1016/j.foreco.2009.09.001

Anderegg WRL, Konings AG, Trugman AT, Yu K, Bowling DR, Gabbitas R, Karp DS, Pacala S, Sperry JS, Sulman BN, *et al.* Hydraulic diversity of forests regulates ecosystem resilience during drought. *Nature* 2018:561(7724):538–541. https://doi.org/10.1038/s41586-018-0539-7

Archie GE. The electrical resistivity log as an aid in determining some reservoir characteristics. *Trans AIME*. 1942:146(01):54–62. https://doi.org/10.2118/942054-G

Bates D, Mächler M, Bolker B, Walker S, Christensen RHB, Singmann H, Dai B, Scheipl F, Grothendieck G, Green P, *et al.* Fitting linear

mixed-effects models using lme4. *J Stat Softw*. 2015:67(1):1–48. https://doi.org/10.18637/jss.v067.i01

Bello J, Hasselquist NJ, Vallet P, Kahmen A, Perot T, Korboulewsky N. Complementary water uptake depth of *Quercus petraea* and *Pinus sylvestris* in mixed stands during an extreme drought. *Plant Soil*. 2019:437(1–2):93–115. https://doi.org/10.1007/s11104-019-03951-z

Billon LM, Blackman CJ, Cochard H, Badel E, Hitmi A, Cartailler J, Souchal R, Torres-Ruiz JM. The DroughtBox: a new tool for phenotyping residual branch conductance and its temperature dependence during drought. *Plant Cell Environ*. 2020:43(6):1584–1594. https://doi.org/10.1111/pce.13750

Blanchy G, Saneiyan S, Boyd J, McLachlan P, Binley A. ResIPy, an intuitive open source software for complex geoelectrical inversion/modeling. *Comput Geosci*. 2020:137:104423. https://doi.org/10.1016/j.cageo.2020.104423

Breshears D, Adams H, Eamus D, McDowell N, Law D, Will R, Williams A, Zou C. The critical amplifying role of increasing atmospheric moisture demand on tree mortality and associated regional die-off. *Front Plant Sci*. 2013:4:266. https://doi.org/10.3389/fpls.2013.00266

Carsel RF, Parrish RS. Developing joint probability distributions of soil water retention characteristics. *Water Resour Res*. 1988:24(5):755–769. https://doi.org/10.1029/WR024i005p00755

Choat B, Brodribb TJ, Brodersen CR, Duursma RA, López R, Medlyn BE. Triggers of tree mortality under drought. *Nature* 2018:558-(7711):531–539. https://doi.org/10.1038/s41586-018-0240-x

Cochard H, Pimont F, Ruffault J, Martin-StPaul N. SurEau: a mechanistic model of plant water relations under extreme drought. *Ann For Sci*. 2021:78(2):1–23. https://doi.org/10.1007/s13595-021-01067-y

Cruiziat P, Cochard H, Améglio T. Hydraulic architecture of trees: main concepts and results. *Ann For Sci*. 2002:59(7):723–752. https://doi.org/10.1051/forest:2002060

Cuneo IF, Knipfer T, Brodersen CR, McElrone AJ. Mechanical failure of fine root cortical cells initiates plant hydraulic decline during drought. *Plant Physiol*. 2016:172(3):1669–1678. https://doi.org/10.1104/pp.16.00923

Dane JH, Topp CG. Methods of soil analysis, part 4: physical methods. New York: John Wiley & Sons; 2020.

de-Dios-García J, Pardos M, Calama R. Interannual variability in competitive effects in mixed and monospecific forests of Mediterranean stone pine. *For Ecol Manag*. 2015:358:230–239. https://doi.org/10.1016/j.foreco.2015.09.014

Delzon S. New insight into leaf drought tolerance. *Funct Ecol*. 2015:29-(10):1247–1249. https://doi.org/10.1111/1365-2435.12500

de Mendiburu F. Agricolae: statistical procedures for agricultural research. *CRAN*. 2023. https://cran.r-project.org/web/packages/agricolae/agricolae.pdf

Domec J-C, King JS, Carmichael MJ, Overby AT, Wortemann R, Smith WK, Miao G, Noormets A, Johnson DM. Aquaporins, and not changes in root structure, provide new insights into physiological responses to drought, flooding, and salinity. *J Exp Bot*. 2021:72(12):4489–4501. https://doi.org/10.1093/jxb/erab100

Duddek P, Carminati A, Koebernick N, Ohmann L, Lovric G, Delzon S, Rodriguez-Dominguez CM, King A, Ahmed MA. The impact of drought-induced root and root hair shrinkage on root–soil contact. *Plant Physiol*. 2022:189(3):1232–1236. https://doi.org/10.1093/plphys/kiac144

Forrester DI, Bauhus J. A review of processes behind diversity—productivity relationships in forests. *Curr Forestry Rep*. 2016:2(1):45–61. https://doi.org/10.1007/s40725-016-0031-2

Grossiord C. Having the right neighbors: how tree species diversity modulates drought impacts on forests. *New Phytol*. 2020:228(1):42–49. https://doi.org/10.1111/nph.15667

Grossiord C, Gessler A, Granier A, Pollastrini M, Bussotti F, Bonal D. Interspecific competition influences the response of oak transpiration to increasing drought stress in a mixed Mediterranean forest. *For Ecol Manag*. 2014a:318:54–61. https://doi.org/10.1016/j.foreco.2014.01.004

Grossiord C, Granier A, Ratcliffe S, Bouriaud O, Bruelheide H, Chećko E, Forrester DI, Dawud SM, Finér L, Pollastrini M, *et al*. Tree diversity does not always improve resistance of forest ecosystems to drought. *Proc Natl Acad Sci*. 2014b:111(41):14812–14815. https://doi.org/10.1073/pnas.1411970111

Grossiord C, Sevanto S, Bonal D, Borrego I, Dawson TE, Ryan M, Wang W, McDowell NG. Prolonged warming and drought modify belowground interactions for water among coexisting plants. *Tree Physiol*. 2019:39(1):55–63. https://doi.org/10.1093/treephys/tpy080

Haberstroh S, Werner C. The role of species interactions for forest resilience to drought. *Plant Biol*. 2022:24(7):1098–1107. https://doi.org/10.1111/plb.13415

Jose S, Williams R, Zamora D. Belowground ecological interactions in mixed-species forest plantations. *For Ecol Manag*. 2006:233:231–239. https://doi.org/10.1016/j.foreco.2006.05.014

Klein T. The variability of stomatal sensitivity to leaf water potential across tree species indicates a continuum between isohydric and anisohydric behaviours. *Funct Ecol*. 2014:28(6):1313–1320. https://doi.org/10.1111/1365-2435.12289

Lebourgeois F, Gomez N, Pinto P, Mérian P. Mixed stands reduce *Abies alba* tree-ring sensitivity to summer drought in the Vosges mountains, western Europe. *Forest Ecol Manag*. 2013:303:61–71. https://doi.org/10.1016/j.foreco.2013.04.003

Leonova A, Heger A, Vásconez Navas LK, Jensen K, Reisdorff C. Fine root mortality under severe drought reflects different root distribution of *Quercus robur* and *Ulmus laevis* trees in hardwood floodplain forests. *Trees* 2022:36(3):1105–1115. https://doi.org/10.1007/s00468-022-02275-3

Liu Z, Ye L, Jiang J, Liu R, Xu Y, Jia G. Increased uptake of deep soil water promotes drought resistance in mixed forests. *Plant Cell Environ*. 2023:46(11):3218–3228. https://doi.org/10.1111/pce.14642

López R, Cano FJ, Martin-StPaul NK, Cochard H, Choat B. Coordination of stem and leaf traits define different strategies to regulate water loss and tolerance ranges to aridity. *New Phytol*. 2021:230(2):497–509. https://doi.org/10.1111/nph.17185

Martin-StPaul N, Delzon S, Cochard H. Plant resistance to drought depends on timely stomatal closure. *Ecol Lett*. 2017:20(11):1437–1447. https://doi.org/10.1111/ele.12851

Mas E, Cochard H, Deluigi J, Didion-Gency M, Martin-StPaul N, Morcillo L, Valladares F, Vilagrosa A, Grossiord C. Interactions between beech and oak seedlings can modify the effects of hotter droughts and the onset of hydraulic failure. *New Phytol*. 2024:241(3):1021–1034. https://doi.org/10.1111/nph.19358

Mencuccini M. The ecological significance of long-distance water transport: short-term regulation, long-term acclimation and the hydraulic costs of stature across plant life forms. *Plant Cell Environ*. 2003:26(1):163–182. https://doi.org/10.1046/j.1365-3040.2003.00991.x

Merlin M, Perot T, Perret S, Korboulewsky N, Vallet P. Effects of stand composition and tree size on resistance and resilience to drought in sessile oak and Scots pine. *For Ecol Manag*. 2015:339:22–33. https://doi.org/10.1016/j.foreco.2014.11.032

Messier C, Bauhus J, Sousa-Silva R, Auge H, Baeten L, Barsoum N, Bruelheide H, Caldwell B, Cavender-Bares J, Dhiedt E, *et al*. For the sake of resilience and multifunctionality, let's diversify

planted forests! *Conserv Lett*. 2022:15:e12829. https://doi.org/10.1111/conl.12829

Moreno M. Influence de la plasticité phénotypique et du mélange d'espèces sur la vulnérabilité hydraulique de forêts méditerranéennes (PhD thesis). Aix-en-provence: Aix-Marseille; 2022. https://theses.fr/2022AIXM0239

Moreno M, Simioni G, Cailleret M, Ruffault J, Badel E, Carrière S, Davi H, Gavinet J, Huc R, Limousin J-M, *et al*. Consistently lower sap velocity and growth over nine years of rainfall exclusion in a Mediterranean mixed pine-oak forest. *Agric For Meteorol*. 2021:308–309:108472. https://doi.org/10.1016/j.agrformet.2021.108472

Nobel PS, Sanderson J. Rectifier-like activities of roots of two desert succulents. *J Exp Bot*. 1984:35(5):727–737. https://doi.org/10.1093/jxb/35.5.727

North GB, Nobel PS. Drought-induced changes in soil contact and hydraulic conductivity for roots of *Opuntia ficus-indica* with and without rhizosheaths. *Plant Soil*. 1997:191(2):249–258. https://doi.org/10.1023/A:1004213728734

Pangle RE, Hill JP, Plaut JA, Yepez EA, Elliot JR, Gehres N, McDowell NG, Pockman WT. Methodology and performance of a rainfall manipulation experiment in a piñon–juniper woodland. *Ecosphere* 2012:3(4):art28. https://doi.org/10.1890/ES11-00369.1

Plaut JA, Yepez EA, Hill J, Pangle R, Sperry JS, Pockman WT, Mcdowell NG. Hydraulic limits preceding mortality in a piñon–juniper woodland under experimental drought. *Plant Cell Environ*. 2012:35(9):1601–1617. https://doi.org/10.1111/j.1365-3040.2012.02512.x

Rodriguez-Dominguez CM, Forner A, Martorell S, Choat B, Lopez R, Peters JMR, Pfautsch S, Mayr S, Carins-Murphy MR, McAdam SAM, *et al*. Leaf water potential measurements using the pressure chamber: synthetic testing of assumptions towards best practices for precision and accuracy. *Plant Cell Environ*. 2022:45(7):2037–2061. https://doi.org/10.1111/pce.14330

Ruffault J, Limousin J-M, Pimont F, Dupuy J-L, De Càceres M, Cochard H, Mouillot F, Blackman CJ, Torres-Ruiz JM, Parsons RA, *et al*. Plant hydraulic modelling of leaf and canopy fuel moisture content reveals increasing vulnerability of a Mediterranean forest to wildfires under extreme drought. *New Phytol*. 2023:237(4):1256–1269. https://doi.org/10.1111/nph.18614

Ruffault J, Martin-StPaul N. Ecopysiological and fuel moisture content data from an experimental drought study on Pinus halepensis and Quercus ilex. France: Recherche Data Gouv; 2024. https://doi.org/10.5774

Ruffault J, Pimont F, Cochard H, Dupuy J-L, Martin-StPaul NK. SurEau-Ecos v2.0: a trait-based plant hydraulics model for simulations of plant water status and drought-induced mortality at the ecosystem level. *Geosci Model Dev*. 2022:15:5593–5626. https://doi.org/10.5194/gmd-15-5593-2022

Ruiz-Benito P, Ratcliffe S, Jump AS, Gómez-Aparicio L, Madrigal-González J, Wirth C, Kändler G, Lehtonen A, Dahlgren J, Kattge J, *et al*. Functional diversity underlies demographic responses to environmental variation in European forests. *Glob Ecol Biogeogr*. 2017:26(2):128–141. https://doi.org/10.1111/geb.12515

Sanchez-Martinez P, Mencuccini M, García-Valdés R, Hammond WM, Serra-Diaz JM, Guo W-Y, Segovia RA, Dexter KG, Svenning J-C, Allen C, *et al*. Increased hydraulic risk in assemblages of woody plant species predicts spatial patterns of drought-induced mortality. *Nat Ecol Evol*. 2023:7(10):1620–1632. https://doi.org/10.1038/s41559-023-02180-z

Schnabel F, Liu X, Kunz M, Barry KE, Bongers FJ, Bruelheide H, Fichtner A, Härdtle W, Li S, Pfaff C-T, *et al*. Species richness stabilizes productivity via asynchrony and drought-tolerance diversity in a large-scale tree biodiversity experiment. *Sci Adv*. 2021:7(51):eabk1643. https://doi.org/10.1126/sciadv.abk1643

Senf C, Buras A, Zang CS, Rammig A, Seidl R. Excess forest mortality is consistently linked to drought across Europe. *Nat Commun*. 2020:11(1):6200. https://doi.org/10.1038/s41467-020-19924-1

Sergent AS, Varela SA, Barigah TS, Badel E, Cochard H, Dalla-Salda G, Delzon S, Fernández ME, Guillemot J, Gyenge J, *et al*. A comparison of five methods to assess embolism resistance in trees. *For Ecol Manag*. 2020:468:118175. https://doi.org/10.1016/j.foreco.2020.118175

Sun Z, Liu X, Schmid B, Bruelheide H, Bu W, Ma K. Positive effects of tree species richness on fine-root production in a subtropical forest in SE-China. *J Plant Ecol*. 2017:10(1):146–157. https://doi.org/10.1093/jpe/rtw094

Ter-Mikaelian MT, Parker WC. Estimating biomass of white spruce seedlings with vertical photo imagery. *New Forests* 2000:20(2):145–162. https://doi.org/10.1023/A:1006716406751

Trogisch S, Liu X, Rutten G, Xue K, Bauhus J, Brose U, Bu W, Cesarz S, Chesters D, Connolly J, *et al*. The significance of tree-tree interactions for forest ecosystem functioning. *Basic Appl Ecol*. 2021:55:33–52. https://doi.org/10.1016/j.baae.2021.02.003

Tyree MT, Ewers FW. The hydraulic architecture of trees and other woody plants. *New Phytol*. 1991:119(3):345–360. https://doi.org/10.1111/j.1469-8137.1991.tb00035.x

Tyree MT, Sperry JS. Vulnerability of xylem to cavitation and embolism. *Annu Rev Plant Physiol Plant Mol Biol*. 1989:40(1):19–36. https://doi.org/10.1146/annurev.pp.40.060189.000315

van Genuchten MT. A closed-form equation for predicting the hydraulic conductivity of unsaturated soils. *Soil Sci Soc Am J*. 1980:44(5):892–898. https://doi.org/10.2136/sssaj1980.03615995004400050002x

Vitali V, Forrester DI, Bauhus J. Know your neighbours: drought response of Norway spruce, silver fir and Douglas fir in mixed forests depends on species identity and diversity of tree neighbourhoods. *Ecosystems* 2018:21(6):1215–1229. https://doi.org/10.1007/s10021-017-0214-0

Wambsganss J, Beyer F, Freschet GT, Scherer-Lorenzen M, Bauhus J. Tree species mixing reduces biomass but increases length of absorptive fine roots in European forests. *J Ecol*. 2021:109(7):2678–2691. https://doi.org/10.1111/1365-2745.13675

Waxman MH, Smits LJM. Electrical conductivities in oil-bearing shaly sands. *Soc Pet Eng J*. 1968:8(02):107–122. https://doi.org/10.2118/1863-A